ISTITUTO NAZIONALE DI FISICA NUCLEARE

INFN/BE - 68/5
28 Giugno 1968

L. Granata and M. Lagonegro:

A PROGRAMME FOR THE COMPUTATION OF THE CORRELATED BEAM OF NEUTRONS FROM THE $T(d,n)He^4$ REACTION WITH A THICK TARGET OF TITANIUM TRITIDE AND COMPARISON WITH THE EXPERIMENTAL RESULTS

A PROGRAMME FOR THE COMPUTATION OF THE CORRELATED BEAM OF NEUTRONS FROM THE $T(d,n)He^4$ REACTION WITH A THICK TARGET OF TITANIUM TRITIDE AND COMPARISON WITH THE EXPERIMENTAL RESULTS

L. Granata and M. Lagonegro

Istituto di Fisica dell'Università di Trieste

1. - INTRODUCTION

The monochromaticity of a neutron beam, produced with a charged-particle reaction, is more or less lost, when, for intensity considerations, one uses a thick target and detectors of finite dimensions [4].

In fact, the degradation of the incident beam of charged particles in the target material and the finite geometry of the detectors are two important factors which influence the energy resolution of the emitted neutrons.

The purpose of this report is to describe a method for calculating the energy spread and the angular spread, caused by a thick target, of the neutrons emitted in the reaction $T(d,n)He^4$.

In addition, the calculation gives the number of neutrons (correlated neutrons) which are associated with the α-particles emitted in a fixed solid angle, relative to the total number of neutrons that have the same spatial directions of the correlated neutrons: all of these neutrons belong to the same cone (neutron cone) relative to the cone of the associated nuclei counted.

2. - GENERAL REMARKS OF THE CALCULATION

One starts from considering an incident beam of charged particles, consisting of monoatomic ions of well defined energy, that strikes a target containing the target nuclei, i.e., nuclei which may undergo the desired neutron-producing reaction, absorbed in a metal.

Let be:

$\left(\frac{dE}{dx}\right)_i$ the rate of energy loss of the incident ions in the target, due to the target nuclei (i=1) and to the metal (i=2) (KeV/mg/cm^2);

ρ_i the density of the target nuclei (i=1) and of the metal (i=2) in the target (mg/cm^3);

$\rho_{tot} = \rho_1 + \rho_2$ (mg/cm^3);

N_i the number of the target nuclei (i=1) and of the metal atoms (i=2) contained in the target, (cm^{-2});

x the thickness of the target (cm);

$\sigma(E)$ the cross-section for neutron production (cm^2);

$\eta = \frac{N_1}{N_2}$ the ratio of the target nuclei to the metal atoms in the target;

$N_L = \frac{N_1}{x}$ the concentration of the target nuclei in the target (cm^{-3}).

Following E.M. Gunnersen et al. ([1]), we may write:

$$\frac{dE}{dx} = \frac{48}{48+3\eta}\left(\frac{dE}{dx}\right)_2 + \frac{3\eta}{48+3\eta}\left(\frac{dE}{dx}\right)_1$$

The thickness dx that corresponds to a decrement dE of the deuteron energy is given by the relation:

$$dx = \frac{dE}{(dE/dx)_{TiT}}\ (\rho_{tot})^{-1}$$

where $(dE/dx)_{TiT}$ is a function of the deuteron energy.

The incident charged particles are absorbed in the target as they undergo the neutron-producing reaction and reach the depth x with a probability

$$T(E,x) = e^{-N_L \int_0^x \sigma(E)dx} = e^{-\frac{N_L}{\rho_{tot}}\int_{E_0}^{E} \frac{\sigma(E)}{(dE/dx)_{TiT}} dE} .$$

Then, they are absorbed within x and x+dx with the probability

$$A(E,dx) = 1 - e^{-N_L\,\sigma(E)\,dx} .$$

Therefore, the total probability for absorption in the target will be:

$$A_{tot} = 1 - e^{-\frac{N_L}{\rho_{tot}} \int_{E_0}^{E_f} \frac{\sigma(E)}{(dE/dx)_{TiT}} dE} .$$

The fraction of neutron-producing reactions taking place within dx is given by

$$P(E,dx) = \frac{\left[e^{-\frac{N_L}{\rho_{tot}} \int_{E(x)}^{E(x+dx)} \frac{\sigma(E)}{(dE/dx)_{TiT}} dE} \times \left(1-e^{-N_L\,\sigma(E)dx} \right) \right]}{A_{tot}\,(E)}$$

where the quantity E_f represents the least energy that contributes to the reaction. In the case of an exothermic reaction, it is $E_f = 0$ if the thickness of the target is greater than the range of the incident particles.

All the equations given above will be now specialized for the case of the reaction $T(d,n)He^4$ and numerically solved.

3.1 COMPUTING PROGRAM FOR THE $T(d,n)He^4$ REACTION

Deuterons of energy ED(1) are incident on a target of tritium absorbed in Ti metal at a 45° angle with respect to the target face.

The deuterons can either react with the tritium nuclei to produce 14 MeV neutrons or be stopped by the titanium. In the last case, the deuterons can undergo the $D(d,n)He^3$ reaction with the incident deuterons and produce neutrons with energy of the order of 2.6 MeV and associated He^3 particles with energy of the order of 750 KeV. In the experimental conditions that will be supposed in the following, the He^3 nuclei have too low an energy in order to be detected. Therefore, only the $T(d,n)He^4$ reaction will be discussed.

We will now give the expressions of the quantities used in the computer program and their symbols:

$\left(\frac{dE}{dx}\right)_1$ = rate of energy loss of the deuterons (in KeV/mg/cm^2) due to the tritium in the target = DEX1(I);

$\left(\frac{dE}{dx}\right)_2$ = rate of energy loss of the deuterons (in KeV/mg/cm^2) due to the titanium in the target = DEX2(I);

ρ_1 = density of the tritium in the target (in mg/cm^2) = RO1;

ρ_2 = density of the titanium in the target (in mg/cm^2) = RO2;

N_1 = number of tritium atoms contained in the target = XN1;

N_2 = number of titanium atoms contained in the target = XN2;

x = thickness of the target (in cm) = SPESSO;

σ = total cross-section for the reaction $T(d,n)He^4$ as a function of the deuteron energy = SIGMA.

The quantities DEX1(I), DEX2(I) and SIGMA are indexed with reference to the discrete energy values that the deuterons are supposed to have while penetrating into the target. For convenience of calculation the deuteron energy is supposed to decrease discontinuously by amounts of predetermined width, DE. The decrement DE must be chosen small enough in order that SIGMA can be considered constant therein.

The deuteron energies will be indicated with:

ED(1) ED(2) ...... ED(I) ...... ED(N),

where ED(I) - ED(I-1) = DE.

The values of $\frac{dE}{dx}$ will be indicated with the symbols DEX1 and DEX2:

DEX1(1) DEX1(2) ..... DEX1(I) ..... DEX1(N)

DEX2(1) DEX2(2) ..... DEX2(I) ..... DEX2(N)

and the values of σ with the symbol SIGMA,

SIGMA(1) SIGMA(2) ..... SIGMA(I) ..... SIGMA(N).

Finally we write

$$ROM = \rho_{tot} = \rho_{Ti} + \rho_T$$

The thickness d_I (symbol DI(I)) of the target where the deuteron energy decreases of DE is given by

$$d_I = \frac{DE}{DEX\ M(I)\cdot ROM}\ (cm)\ .$$

The contribution of each DI(I) to the production of neutrons is

$$ASSB(I) = 1 - e^{-N_L\ \sigma_I\ d_I}$$

The probability for a deuteron to reach the layer d_I is:

$$TRASM(I) = e^{-N_L \sum_{1}^{I-1}{}_K\ \sigma_K\ d_K}\ .$$

The total absorption is given by:

$$ASSB_{TOT} = 1 - e^{-N_L \sum_{1}^{n}{}_I\ SIGMA\ (I)DI(I)}\ .$$

The fraction of neutrons produced in each layer is:

$$P(I) = \frac{e^{-N_L \sum_{1}^{I-1}{}_K\ \sigma_K\ d_K}\left(1-e^{-N_L\ \sigma_I\ d_I}\right)}{1-e^{-N_L \sum_{1}^{n}{}_I\ \sigma_I\ d_I}} =$$

$$= \frac{TRASM\ (I-1) \times ASSB\ (I)}{ASSB_{TOT}}$$

where:

$$n = \frac{ED(1)}{DE} = \frac{\text{energy of the incident deuteron}}{\text{energy decrement}}$$

if $\sum_{1}^{n}{}_I\ d_I < x$, while if $\sum_{1}^{n}{}_I\ d_I > x$, n' is substituted for n, where n' is the integer part of the number zn with z defined by:

$$z = \frac{x}{\Sigma_I d_I} \quad .$$

On the base of the relationships given above, the energy degradation of the deuterons in the target and the production of neutrons can be calculated.

To analyze the beam of correlated neutrons, the following method is carried out.

A neutron and an associated α-particle are produced. The α-particle is produced at an angle of $90° \pm \Delta\varphi_\alpha$, (where $\Delta\varphi_\alpha$ is the half-width of the angle subtended by the α-particle detector) with respect to the direction of the incident deuterons. The correlated neutrons are emitted over a spectrum of angles about an angle ϑ_n. The amplitude of this angular interval is determined by $\Delta\varphi_\alpha$, and by the different energies which the deuteron attains in its degradation in the target. Let $\Delta\vartheta_n$, be the half-opening of the neutron cone. In the calculation one considers an interval about the angle ϑ_n, but wider than the predicted value $\Delta\vartheta_n$ and it is divided into k intervals. The kinematics are carried out for the successive values of the deuteron energy. Then, if the α-particle is emitted in the angular interval between $90°-\Delta\varphi_\alpha$ and $90°+\Delta\varphi_\alpha$, the fractional production of neutrons for each deuteron energy is recorded; while no recording is taken if the angle of emission of the α-particle does not belong to the interval specified above. In this way, the following matrix of n rows and k columns is constructed.

$$A(i,k) = \|Pik\|$$

where $Pik = P(I)$ if the neutron emitted in the k-th angular interval corresponds to an α-particle emitted within the cone $90° \pm \Delta\varphi_\alpha$, otherwise $Pik=0$.

Now to obtain the shape of the beam of the correlated neutrons it is sufficient to sum the corresponding Pik elements for each k. The function:

$$SUM(K) = \sum_{1}^{n}{}_I \; Pik$$

gives the fraction of the neutrons emitted at a given angle which are correlated neutrons.

So, by fixing an angular interval belonging to the cone of the correlated neutrons one can determine the ratio

$$\frac{N_{corr}}{N_{non\ corr}}$$

and also the energy spread characterizing the correlated neutrons.

In the case we are considering, it is

ED(I) = 200 KeV
DE = 25 KeV
n = 8
k = 100 (30' intervals from 69° to 118°).

The input data DEX1(I), DEX2(I) and SIGMA(I) are also known and are reported in Table 1.

The data concerning the target are:

activity of the target = 2 Curie/cm^2
N_1 = 6.372×10^{18} atoms/cm^2
N_2 = 4.900×10^{18} atoms/cm^2
η = 1.3
RO2 = 4500 mg/cm^3
RO1 = 382 mg/cm^3
x = 0.870×10^{-4} cm, equivalent to 380 μgr/cm^2 Ti
X(45°) = 1.22×10^{-4} cm.

The programme allows also to calculate the residual energy that the associated α-particles have when they emerge from the target and the corresponding time-of-flight in nsec/m. The loss of energy suffered by the α-particles while passing through the target is calculated with Bloch's formula(2) for both the target components.

The total energy loss due to the mixture is evaluated by using Bragg's formula, already used in the case of the deuterons.

3.2 NUMERICAL RESULTS

The values of the function P(I) are given in Table 2. It can be seen that the greatest contribution comes from deuteron energy values between 100 KeV and 125 KeV, where the cross section of the reaction $T(d,n)He^4$ reaches its maximum value.

In addition to computing the function P(I), the program computes the thickness S that the deuteron must pass through in order to be slowed down from a given energy ED to an energy ED-ΔED, where ΔED = 25 KeV. The values of these thicknesses are given in Table 3; it can be assumed that deuterons of 200 KeV have a range of 0.812 μ.

In Table 4 are listed the values of the absorption of the deuteron beam as it penetrates into the target and undergoes the neutron-producing reaction, along with the values of the neutron yields referred to 1μA of incident beam current.

These yields are compared with experimental yields affected by errors that are due to unavoidable small deflections of the deuteron beam that cause the shifting of the target area struck by the beam. The discrepancies between calculated and measured yields can be attributed to the fact that the incident beam contains also biatomic molecules of deuterium. The results obtained for the P(I), the deuteron range, the ASSB(I) and the yield of neutrons are shown in Figures 1, 7, 8, 9.

The laboratory angular distribution of the neutrons that are associated with the α-particles emitted in the angular intervals measured with respect to the incident beam direction, from 88° to 92°, from 86°30' to 93°30' from 80° to 94°, from 84°30' to 95°30' are shown in Figures 3, 4, 5, 6. These graphs represent the function SUM(K) and are tabulated in Table 5.

The values of the mean energy and of the energy spread of the neutrons which are associated with the α-particles counted in the solid angles given above are reported in Table 6.

From the preceding graphs, one can see that by varying the width of the angle including the directions of the detected α-particles, it changes the spectrum of angles over which the correlated neutrons are produced as well as the spectrum of angles over which one may count 100 per cent of correlated neutrons. One may also notice that the neutron energy spread increases by opening the cone containig the 100 percent of correlated neutrons.

In the following paragraph we will make a comparison between the experimental results and the calculated values relative to the shape of the correlated neutron beam and to the fractional yield of correlated neutrons. In addition, the results of the calculations relative to the α-particles are also reported since they play an important role in the evaluation of the effect due to the electronic bias set in the α-channel.

4. - COMPARISON WITH EXPERIMENTAL RESULTS

The experiments have been carried out with the t.o.f. method.

The α-particles were detected by means of a NE 810 type detector, consisting of a thin sheet of NE 102 A plastic scintillator of thickness 0.03" mounted on a light pipe of thickness 0.1" and coupled with a 56 AVP photomultiplier.

The neutrons were detected using a NE 102 A plastic scintillator, 2" diameter, 1,5" thick, coupled with an XP 1021 photomultiplier.

Two measurements have been performed with $\Delta\varphi_\alpha = 5°35'$ and $\Delta\varphi_\alpha = 1°47'$ respectively.

In the first case the source-to-detector distance was equal to 3 meters. So, the angle subtended from the source to the detector resulted to be equal to 58'. The geometric configuration is shown in Figure 10.

In this condition it has been measured:

- the energy spectrum of the neutrons in coincidence with the associated α-particles, in the angular range from 76° to 93°, by steps of 1°;
- the neutron time-of-flight spectrum in the above angular range, by steps of 2°;

- the energy spectrum of the direct beam of neutrons;
- the energy spectrum of the background in the neutron channel either direct and in coincidence with the α-channel.

In addition it was also measured the background spectrum in the neutron channel after short and long periods of time were elapsed since the start up of the accelerator. Also, spectra in the neutron channel have been registered with the accelerator on but without the tritium target; this was done in order to check if there were any neutron produced by the (D,d) reaction in a self-formed deuterium target in the collimator, 1 meter away from the real target.

Since the neutron detector was displaced along a vertical direction, it was necessary to correct for the variation of the solid angle. The correction resulted not bigger than 1% and was calculated as follows

$$d_n = \frac{d}{\sin \varphi_n}$$

$$S_n = S \sin \varphi_n$$

$$S_n = \frac{S(\sin \varphi_n)^3}{d^3}$$

Therefore the correction factor was given by

$$k = (\sin \varphi_n)^{-3} .$$

The displacement of the neutron detector corresponded to an angular variation of 1 degree. So the scanning was such to allowe a fairly good reproduction of the shape of the beam of correlated neutrons.

The shape of the beam was obtained by counting the (α,n) coincidences for 18 different angular positions of the n-detector between 76° and 93°. The spurious coincidences for each angular position were counted using the t.o.f. method. In such a way, both the distribution of the neutrons effectively associated with the α-particles and an information concerning the number of spurious coincidences were obtained. The difficulty of obtaining a better result regarding the spurious coincidences was due to the lack of uniformity in the rate of the neutron production. The number of the counted spurious coincidences varied between 800 and 1100 in correspondence of the maximum of the beam and from 400 to 800 on the sides of this maximum.

One fact that was observed was that the position of the α-particle detector was not exactly reproduceable. Anyhow, a part from a problem of alignement of the beam, this was not a drawback, since, due to the isotropy of the cross-section of the $T(d,n)He^4$ reaction, all the problems we are concerned with were not affected by it.

In Table 7 are reported the data relative to the beam shape determination.

For the angles for which t.o.f. spectrum measurements have not been performed, the coincidences have been corrected for spurious events by subtracting the average number of spurious events recorded in correspondence of the nearest two angles. The numbers so corrected are written in brackets in the last column of Table 7. These numbers need a final correction due to the fact that about 3% of the α-particles that emerge from the target have not a sufficient energy to be detected. Let us consider the mean energy and the energy spread of the α-particles emerging from the target. The data are reported in Table 8.

In the Table, E_α indicates the mean energy values of the α-particles produced in the reaction; E_α^u indicates the mean energy values of the α-particles that emerge from the target; ΔE_α^u indicates the mean width of the energy spread produced by the thickness passed through. The total spread is approximately double that indicated. To shield the α-particle detector from the light, a layer of aluminium of 800 $\mu g/cm^2$, equal to about 3 μm, is interposed between the target and the detector itself. This causes a reduction of the α-particle energy and a slight increase of the energy spread. After having passed through the shield, the α-particles have the energies reported in Table 9.

About 2 - 2.5% of the α-particles are eliminated by the electronic threshold, which operates at about 400 KeV. Therefore, it is necessary to consider a mean loss of α-particles of a few % due to the electronic threshold and to the absorber interposed in the α-particle channel. The experimental values compared with the theoretical values are shown in Fig. 12.

The measured distribution is shifted by 1 degree to the left to make the comparison clearer: the measurements show that the beam is effectively included between 76° and 93°. The displacement is due to the difficulty in reproducing the alignment of the α-particle detector and corresponds to an angular position of 89° 20' of the detector itself. The uncertainties shown by the points are due to the angular width of the detector and to the preceding considerations.

The agreement between the results of the calculus and the experimental data is fairly good. The beam experimentally determined is narrower than the calculated one since the openning of the cone subtended by the α-particle detector is really equal to 5°15'.

In addition to the determination of the beam shape. the following measurements have been performed at 78° and 84°:

a) measurement of the spectra of neutrons both in coincidence and not;

b) measurement of the background spectra;

c) measurement of spectra without target.

Measurement a) was carried out with the purpose of evaluating the height of the distribution of the neutrons associated with the α-particles relative to the height of the distribution of all the neutrons. So to have a factor for the normalization of the measurements concerning the correlated neutrons and performed in two different positions.

Figures 13 and 14 show the spectrum of all the neutrons and the spectrum of the associated neutrons.

The spectra of the neutrons not in coincidence with the α-particles that have been measured at 78° (Fig. 13) and 84° (Fig. 14) show a discrepancy in a region of channels of low number. The two spectra should be ex pected to be equal a part from small differences introduced by the solid angle.

These differences are partially compensated for by the variation of the order of 2% of the differential cross-section of the reaction $T(d,n)He^4$ in favour of the 78° angle.

The two spectra are seen to coincide from the channel 90 to the channel 160 and are slightly different between the channels 55 and 90.

Neither the background not the virtual (D,d) neutron source can account for the discrepancy, since their spectra measured at 78° and 84° are identical.

The most valid hypothesis is that the discrepancy is due to the activation of the materials contained in the target and of the nearby objects. In fact, if the measurement of the background spectrum is carried out with a lead shadow, 14 cm in diameter and 50 cm long, interposed between the neutron source and the neutron detector, the discrepancy disappears. On the other hand, the effect of the activation is very low in the measurement of the spectrum of neutrons both in coincidence and not performed at 84° and is evident in the measurement performed at 78°. This circumstance can be explained by the fact that in the case of the measurement at 84° the accelerator was just started up while in the case of the measurement at 78° the accelerator was being in use since a couple of hours.

A slight disagreement is also present between the correlated and non-correlated spectrum at 84°. While from channel 90 to 160 the ratio between the two heights varies between 0.95 and 1, below channel 90 the ratio is as low as 0.80. This occurs in the range where the non-correlated spectra at 78° and 84° show a small discrepancy due to effects of the activation of the target and nearby objects.

The shifting between the two spectra (correlated and non-correlated) at 84° can be explained by considering the slight activation present at the beginning of the measurement; while that between the free spectra at 78° and 84° can be attributed to the increase of the activation during the operation of the accelerator.

With these considerations the relative heights of the correlated spectra in respect to the free spectra can be explained. The data are reported in Table 9.

In the present situation the centre of the beam can be assumed to be at the 84° angle. As far as the ratio (correlated neutrons - non-correlated neutrons) that is derived from the spectra at 84° is concerned, it is seen that the only neutrons that do not contribute to the coincidence measurements are those lost by the effect of the electronic threshold. Under these threshold conditions the loss is lower than 5% so that one can assume that the ratio has a value between 0.95 and 1.00.

The spectra measured without the target did not give appreciable results and therefore have not been reported in the text.

Another test regarding only the form of the beam was carried out under different geometric conditions. The distance from the target to the neutron detector was made equal to 167 cm, and $\Delta\varphi_\alpha = 1^\circ 47'$; the angle of detection of the neutrons was varied by approximately 1°20' for each measurement. This test is compared (see Fig. 15) with the theory where $\Delta\varphi_\alpha = 1^\circ 45'$.

As far as the spectra of the α-particles is concerned, Fig. 10 shows the comparison between the results of the calculation and the experimental results obtained with a solid state detector (type ORTEC SBEE-100).

The calculated α-particles energy is the energy with which the α-particles emerge from the target and is computed by means of the Block's formula.

The values of the energy spread of the α-particles take into account both the resolution of the detector system and the effect due to the aluminium adsorber. Altogether this is as high as 130 KeV in this case. It is interesting, however, to notice that the calculated values of the energy and the energy spread disagree with the measured ones within the experimental precision. The spectra are reported in Figs. 16. 17, 18.

Many thanks are due to Prof. G. Poiani for having stimulated the present work, and to Prof. G. Pauli for helpful comments.

* * *

ED (KeV)	DEX1 (KeV/mg/cm^2)	DEX2 (KeV/mg/cm^2)	SIGMA (barn)
200	1211	285	2.50
175	1231	280	3.20
150	1270	276	4.00
125	1292	267	4.90
100	1290	252	5.00
75	1253	228	3.60
50	1128	193	1.40
25	802	132	0.15

Table 1 - Rate of energy lass of deuterons in tritium (DEX1) and in titanium (DEX2). Values of the cross-section for the reaction T(d,n)He^4 (SIGMA)

ED(KeV)	P(I) %
200	9.41
175	12.20
150	15.20
125	19.00
100	20.20
75	15.80
50	7.10
25	1.10

Table 2 - Relative yield of neutrons for different deuteron energies.

ED (KeV)	DI (micron)	range (micron)
200	0.085	0.812
175	0.086	0.727
150	0.086	0.641
125	0.087	0.556
100	0.091	0.468
75	0.098	0.378
50	0.114	0.279
25	0.165	0.165

Table 3 - Values of the thickness DI and of the range of the deuterons in target as a function of the deuteron energy.

ED (KeV)	ASSB(I) (10^6)	Neutron yield(10^{-8})	
		calculated	measured
200	1.55	1.023	1.33 ± 0.4
175	2.00	0.924	
150	2.51	0.800	0.86 ± 0.15
125	3.13	0.645	0.55 ± 0.15
100	3.33	0.453	
75	2.60	0.242	
50	1.17	0.081	
25	0.20	0.012	

Table 4 - Absorption of the deuterons in the target and total neutron yield for different deuteron energies.

φ neutrone	$\Delta\varphi\alpha$ = 2°	$\Delta\varphi\alpha$ = 3°30'	$\Delta\varphi\alpha$ = 4°	$\Delta\varphi\alpha$ = 5°30'
75°30'				9.41
76°				21.60
76°30'			7.59	21.60
77°		7.59	7.59	36.80
77°30'		7.59	18.00	55.80
78°		18.00	32.10	55.80
78°30'	7.59	32.10	50.90	76.00
79°	7.59	50.90	50.90	76.00
79°30'	18.00	50.90	72.40	91.80
80°	32.10	72.40	72.40	91.80
80°30'	50.90	72.40	90.20	98.90
81°	50.90	90.20	90.20	98.90
81°30'	72.40	90.20	98.70	98.90
82°	72.40	98.70	98.70	100.00
82°30'	82.60	98.70	98.70	100.00
83°	82.60	98.70	100.00	100.00
83°30'	80.70	100.00	100.00	100.00
84°	66.60	92.40	100.00	100.00
84°30'	47.80	92.40	92.40	100.00
85°	49.10	82.00	92.40	100.00
85°30'	27.60	67.90	82.00	100.00
86°	27.60	49.10	67.90	100.00
86°30'	9.83	49.10	49.10	100.00
87°	9.83	27.60	49.10	90.60
87°30'	1.30	27.60	27.60	78.40
88°	1.30	9.83	27.60	78.40
88°30'	1.30	9.83	9.83	63.20
89°		1.30	9.83	44.20
89°30'		1.30	1.30	44.20
90°		1.30	1.30	24.00
90°30'			1.30	24.00
91°				8.20
91°30'				8.20
92°				1.10
92°30'				1.10
93°				1.10

Table 5 - Histograms of the correlated neutron beam corresponding to different angles of the α-particle detector.

$\Delta\varphi_\alpha$	<EN> (MeV)	ΔEN (MeV)
2°	14.192	0.253
3° 30'	14.200	0.286
4°	14.192	0.298
5° 30	14.203	0.328

Table 6 - Mean energy and energy spread of the correlated neutrons.

φ_n	number of coincidence counts	time-of-flight counts	time-of-flight spurious counts	geometrical factor k	counts for measured shape
76°	1062	408	431	1.09	445
77°	2333			1.08	(1860)
78°	4142	3785	790	1.07	4050
79°	7374			1.06	(6850)
80°	10327	9154	1027	1.05	9600
81°	12227			1.03	(11700)
82°	13127	11981	864	1.03	12200
83°	14002			1.02	(13300)
84°	14346	13347	1071	1.02	13600
85°	14000			1.01	(13200)
86°	13783	13068	827	1.01	13100
87°	12885			1.01	(12300)
87° 30'	13418	12825	593	1.00	12825
88°	11226			1.00	(10498)
89°	9642			1.00	(8914)
89° 30'	8526	7662	864	1.00	7662
90°	5919			1.00	(5133)
91°	3313			1.00	(2527)
91° 30'	2577	1868	709	1.00	1868
92°	1690			1.00	(1340)
93°	1090			1.00	(740)

Table 7 - Experimental data relative to the beam shape determination for α-particles detected between 84° 30' and 95° 30'.

ED (KeV)	$<E_\alpha^o>$ (MeV)	$<E_\alpha^u>$ (MeV)	$<\Delta E_\alpha^u>$ (MeV)
200	3.50 ± 0.10	3.500	0.200
175	3.50 ± 0.10	3.500	0.190
150	3.50 ± 0.10	3.500	0.160
125	3.50 ± 0.10	3.498	0.150
100	3.53 ± 0.07	3.498	0.130
75	3.54 ± 0.07	3.495	0.110
50	3.55 ± 0.07	3.495	0.100
25	3.54 ± 0.07	3.485	0.070

Table 8 - $<E_\alpha^o>$ = mean energy of the α-particles
$<E_\alpha^u>$ = mean energy of α-particles energing from the target
$<\Delta E_\alpha^u>$ = mean energy spread of α-particles.

ED (KeV)	$<E_\alpha^r>$ (MeV)	$<\Delta E_\alpha^r>$ (MeV)
200	2.700	0.210
175	2.700	0.200
150	2.700	0.170
125	2.698	0.160
100	2.698	0.140
75	2.695	0.124
50	2.695	0.115
25	2.685	0.090

Table 9 - $<E_\alpha^r>$ = residual energy of the α-particles that cross the allu-minium absorber
$<\Delta E_\alpha^r>$ = mean energy spread of α-particles.

φ_n	from neutron spectrometry	from time-of-flight measurements	from computer programme
78°	0.31	0.30	0.32
84°	0.97	0.99	1.00

Table 10 - Calculated and measured values of the ratio:

number of correlated neutron/number of non correlated neutron at 78° and 84°.

ED (KeV)	α-particle energy (MeV)		energy spread (MeV)	
	calculated	measured	calculated	measured
200	2.700	2.820	0.240	0.330
150	2.700	2.839	0.206	0.256
120	2.698	2.839	0.198	0.247

Table 11 - Comparison between the calculated and the measured α-particles energies.

* * *

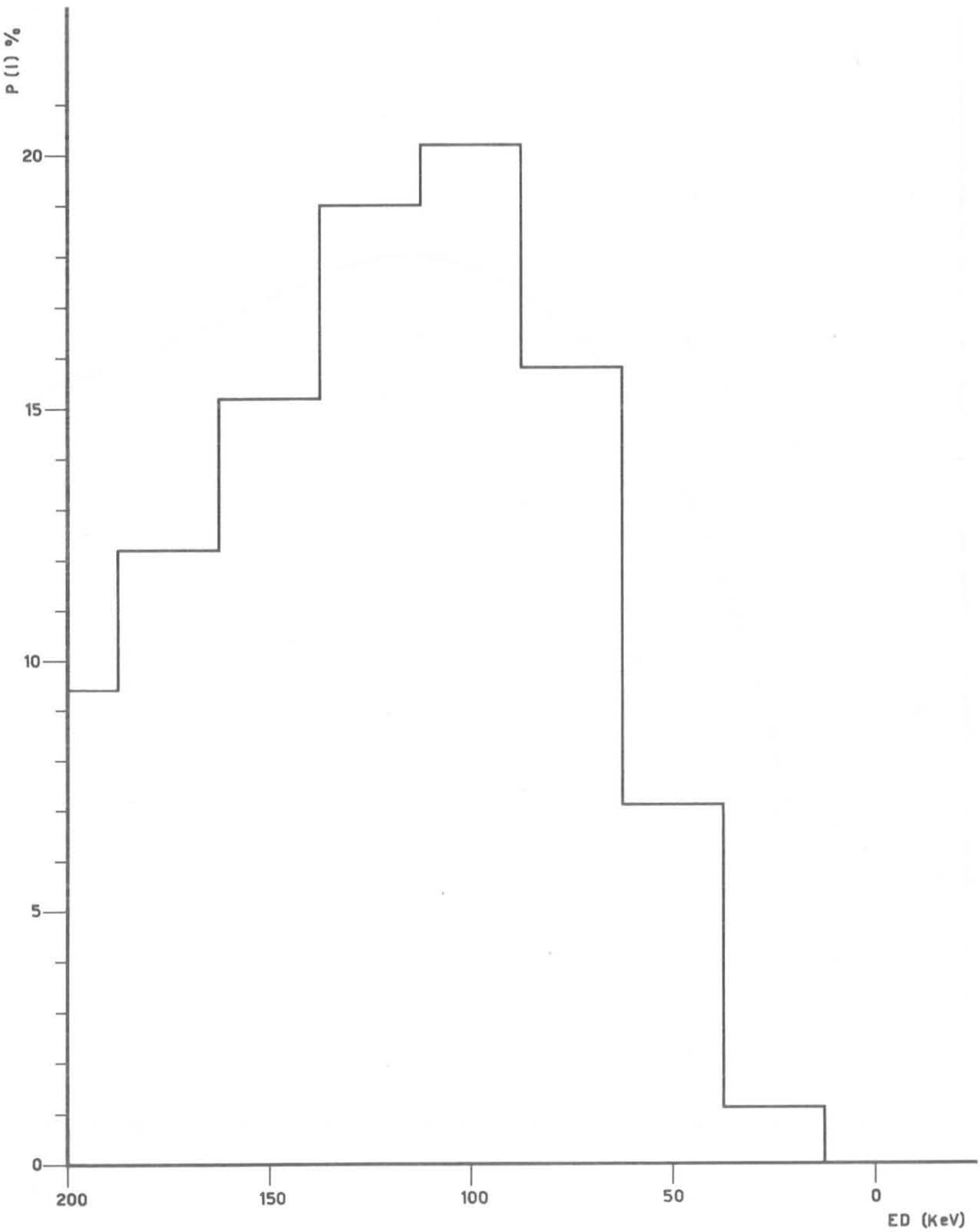

Fig. 1 - Relative yield of neutrons from the $T(d,n)He^4$ reaction for different deuteron energy.

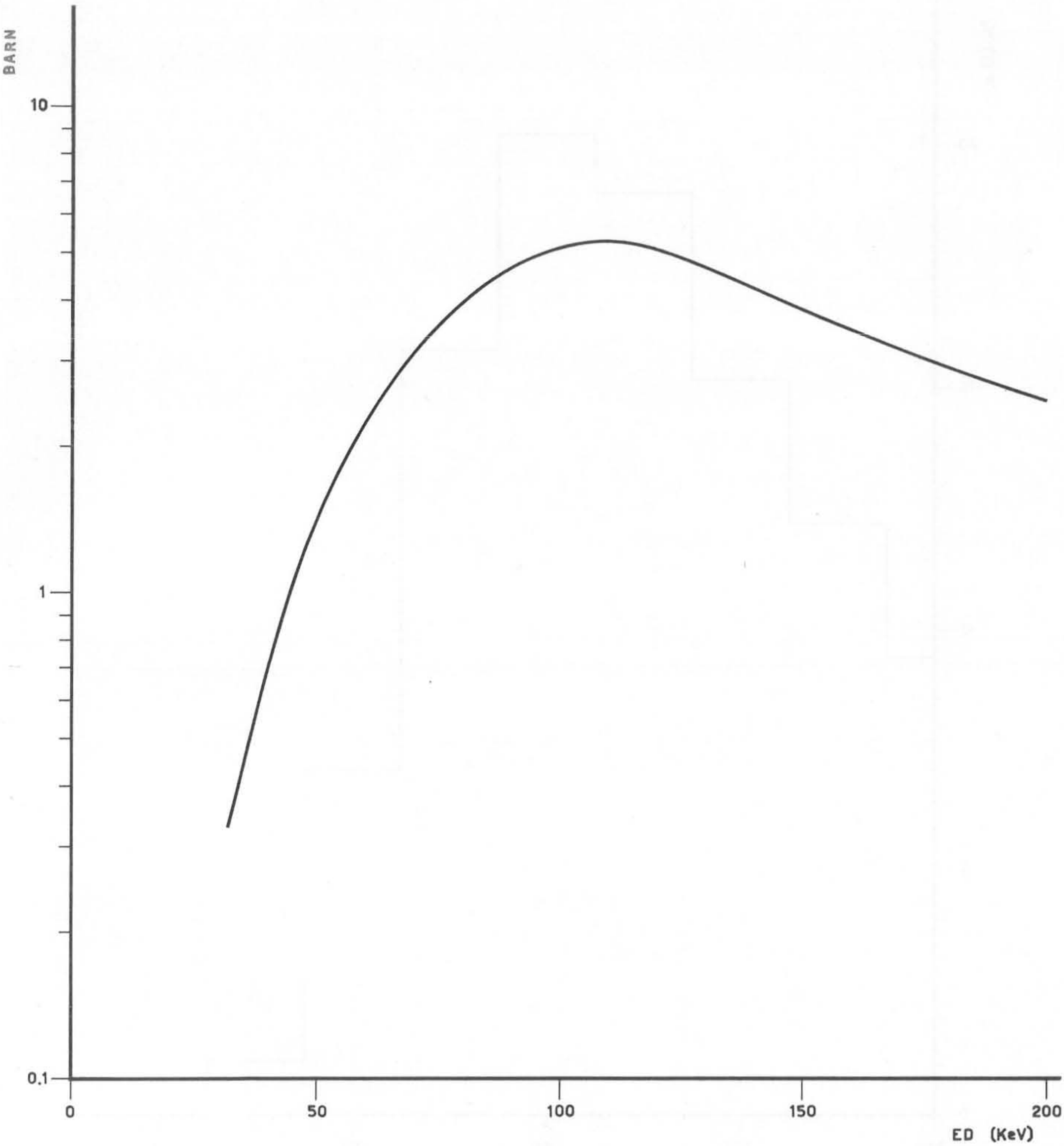

Fig. 2 - Cross-section of the $T(d,n)He^4$ reaction as a function of deuteron energy.

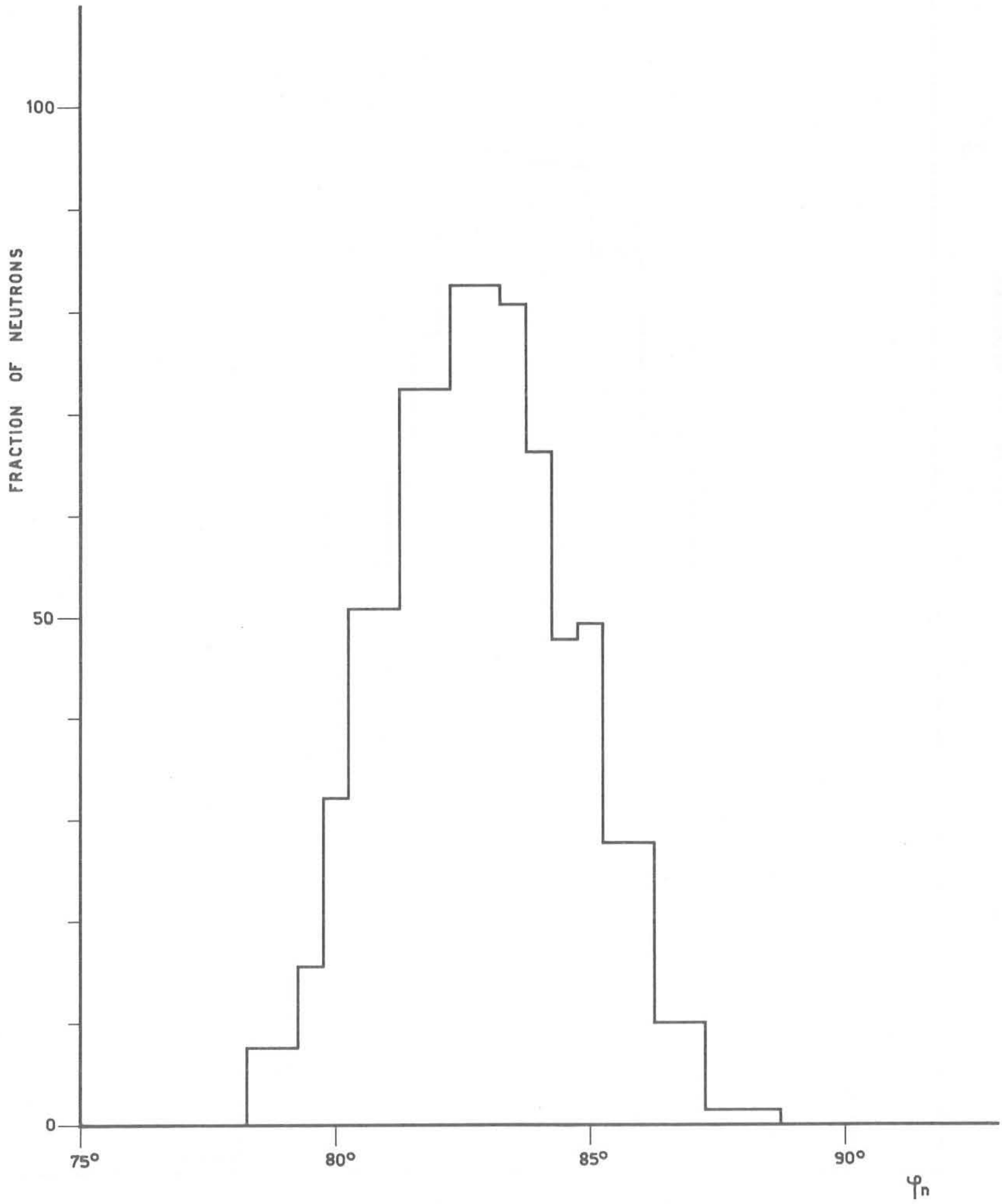

Fig. 3 - Shape of the beam of the neutrons for α-particles emerging between 88° and 92°.

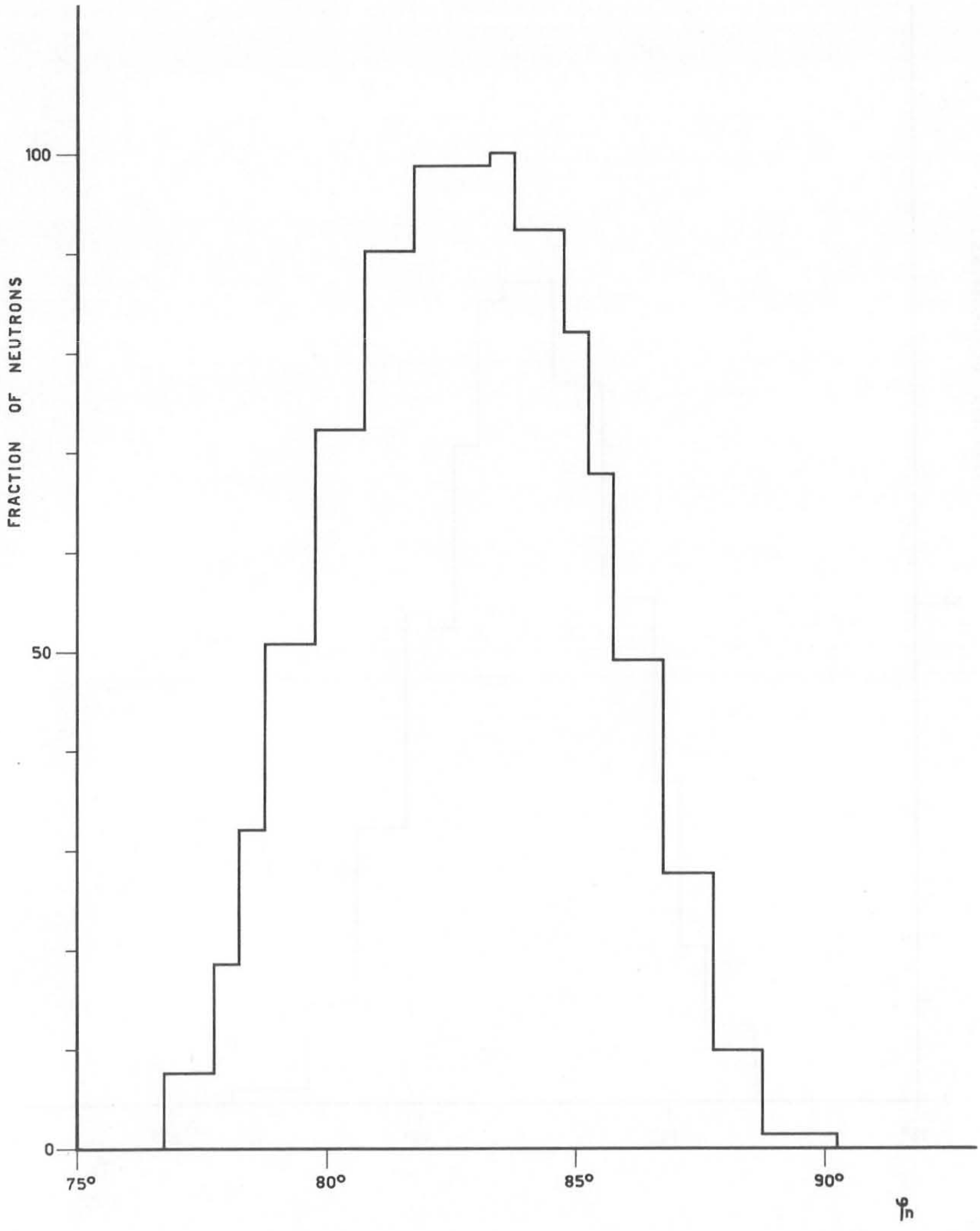

Fig. 4 - Shape of the beam of the neutrons for α-particles emerging between 86° 30' and 93° 30'.

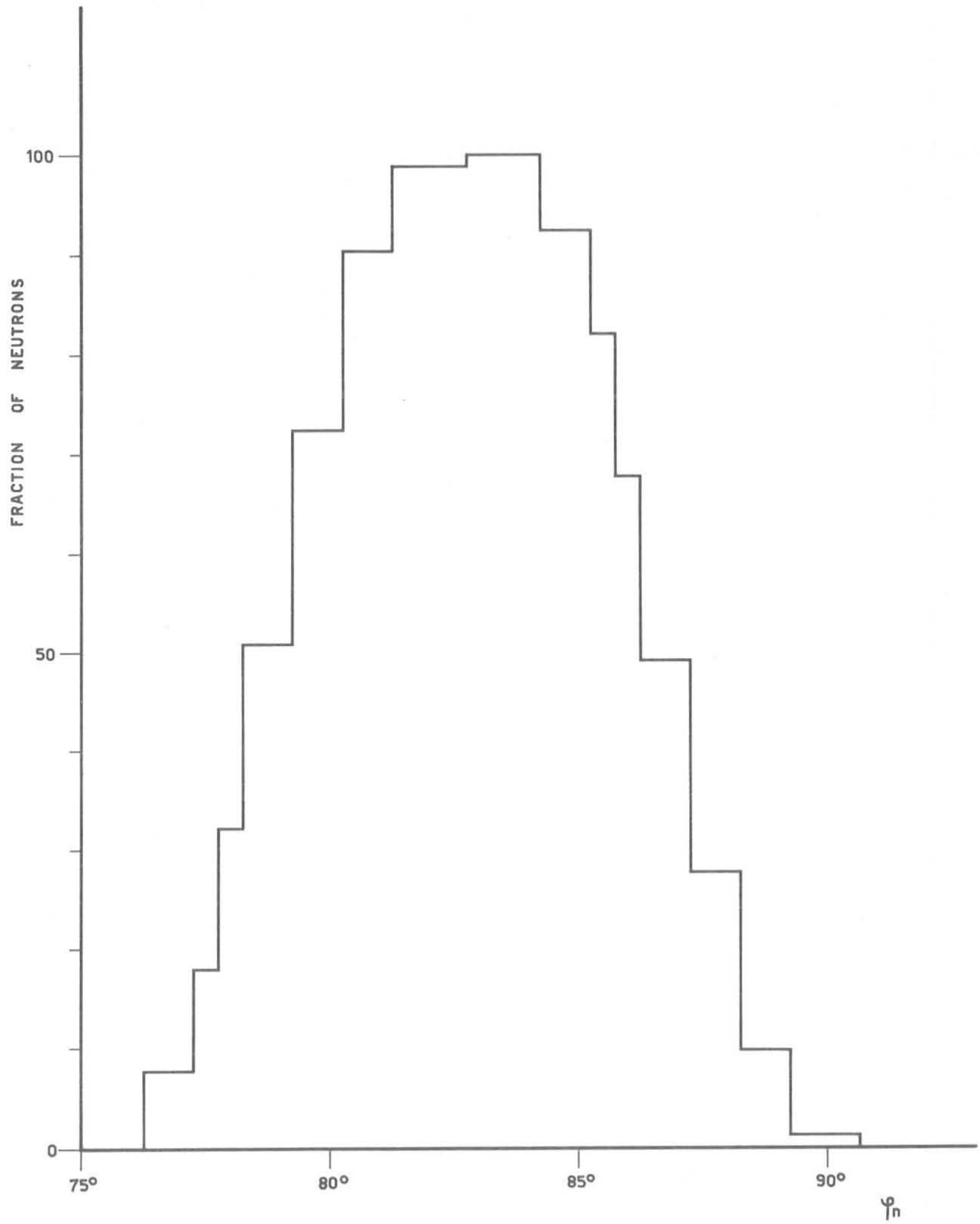

Fig. 5 - Shape of the beam of the neutrons for α-particles emerging between 86° and 94°.

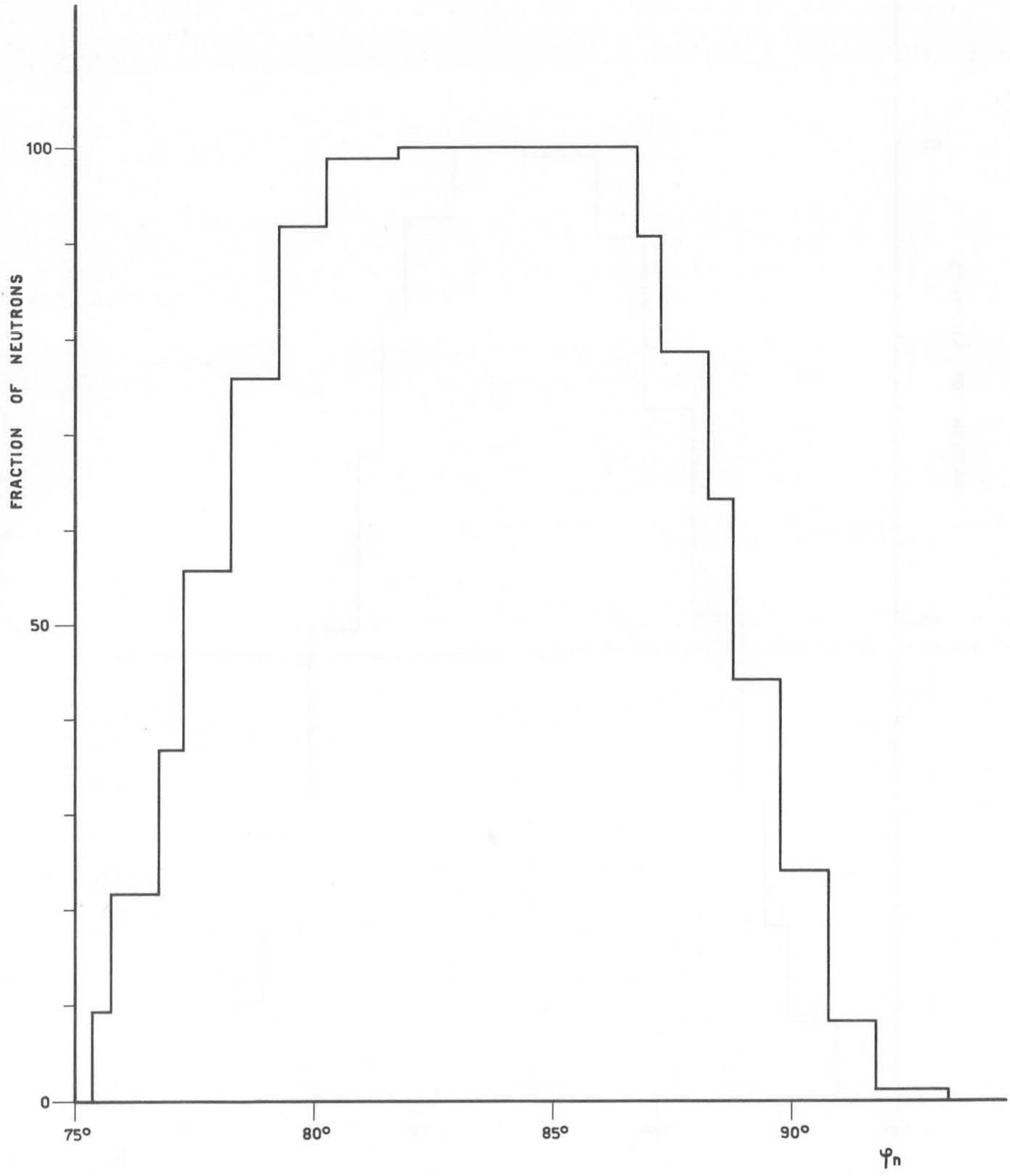

Fig. 6 - Shape of the beam of the neutrons for α-particles emerging between 84°30' and 95°30'.

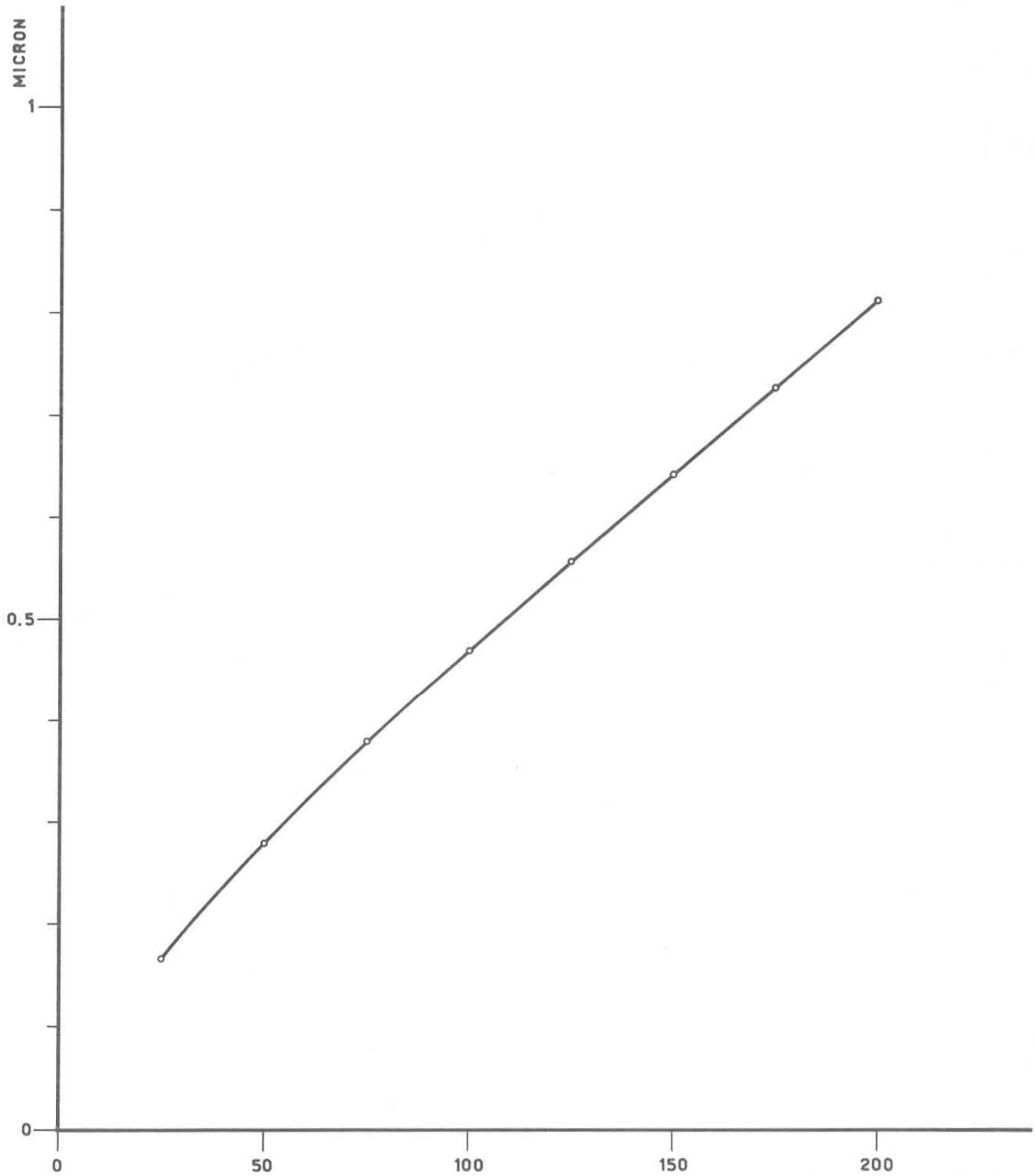

Fig. 7 - Deuterons range in the titanium-tritide target.

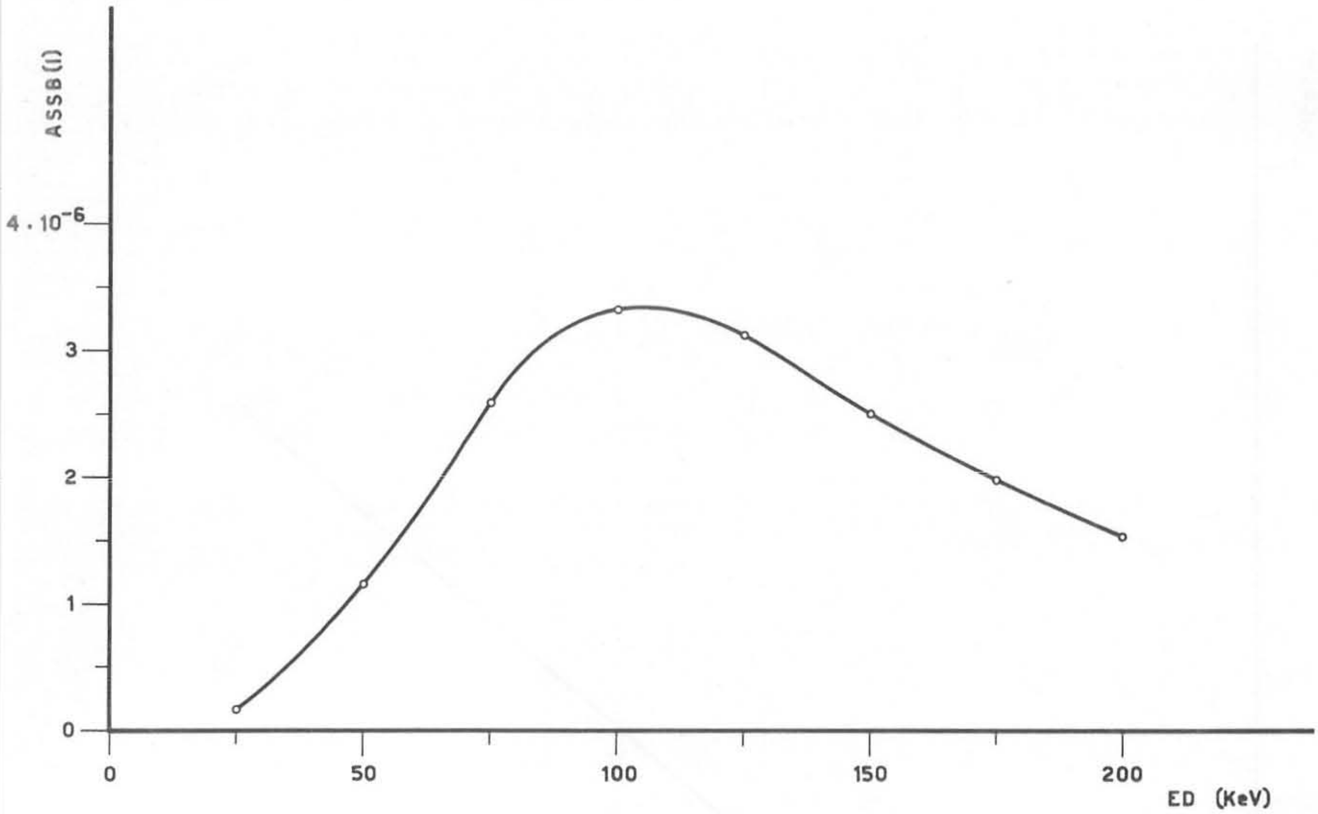

Fig. 8 - Absorption of deuterons of different energies in the thicknesses DI.

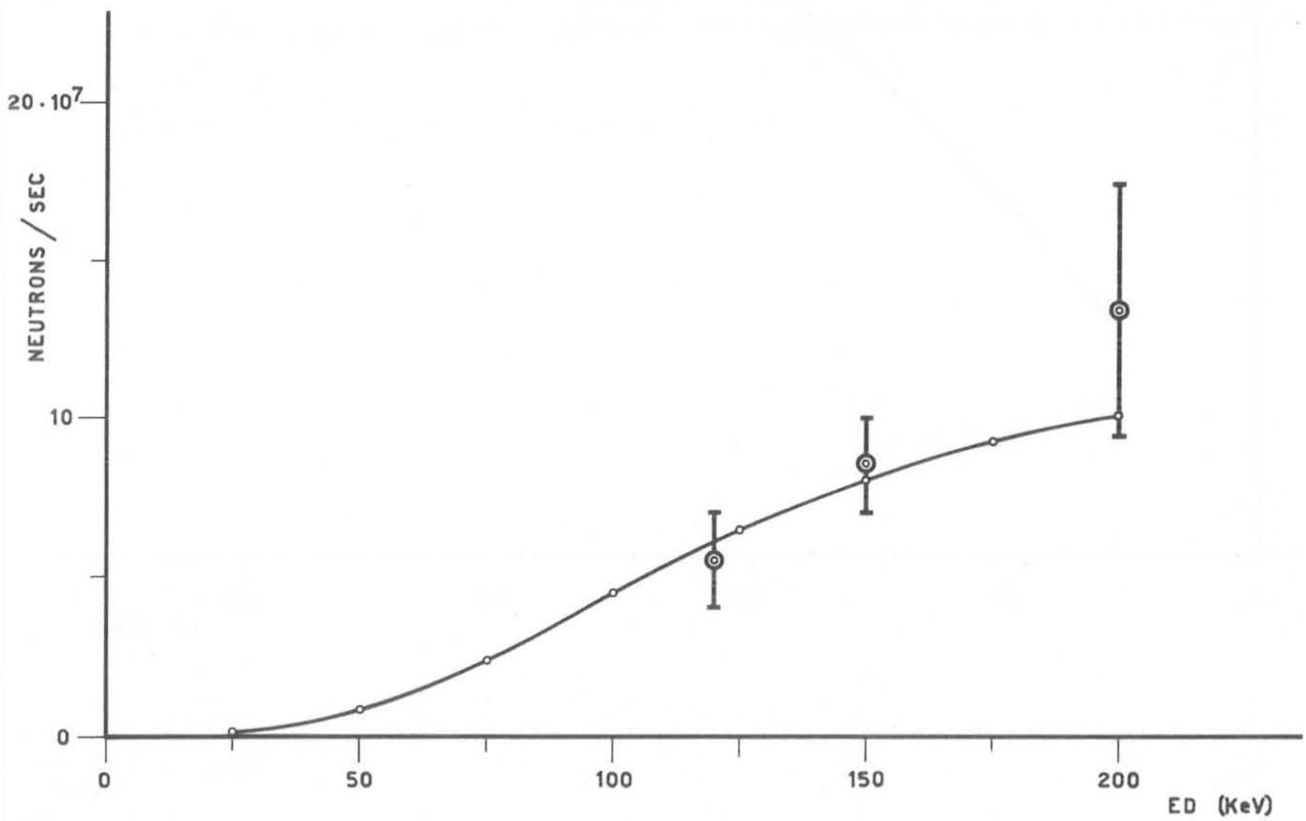

Fig. 9 - Neutron yield for 1 μA of deuteron current striking the target.

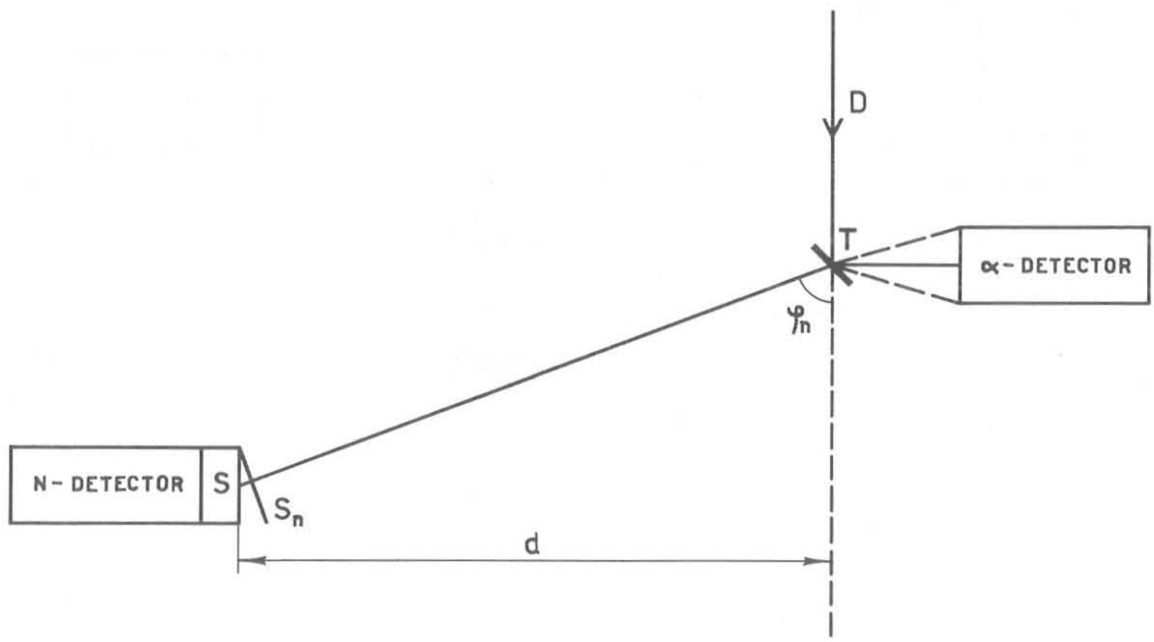

Fig. 10 - Scheme of experimental geometry.

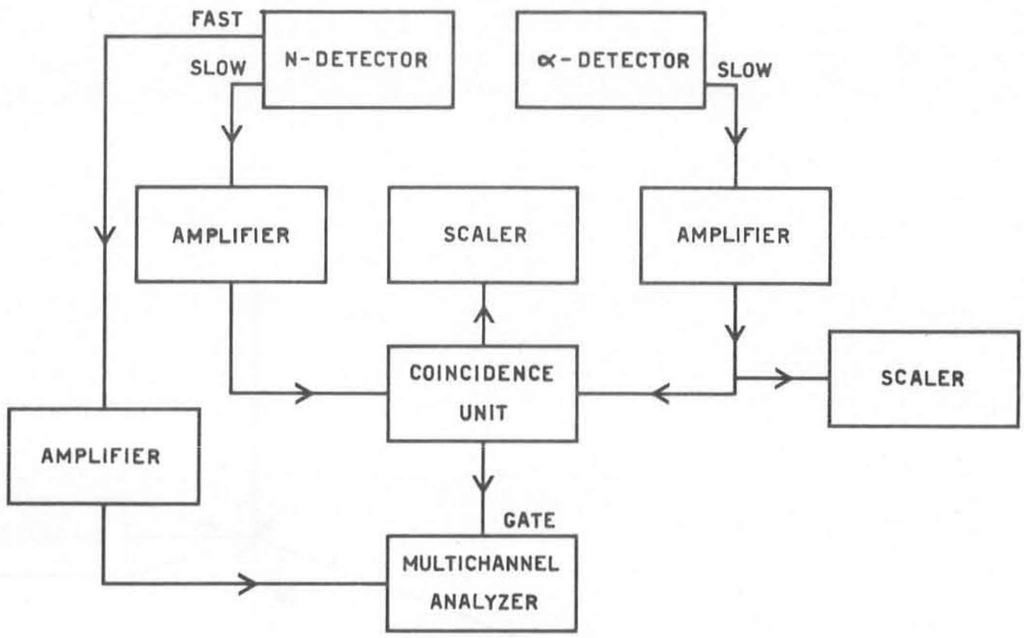

Fig. 11 - a) Block diagram of apparatus for neutrons spectrometry.

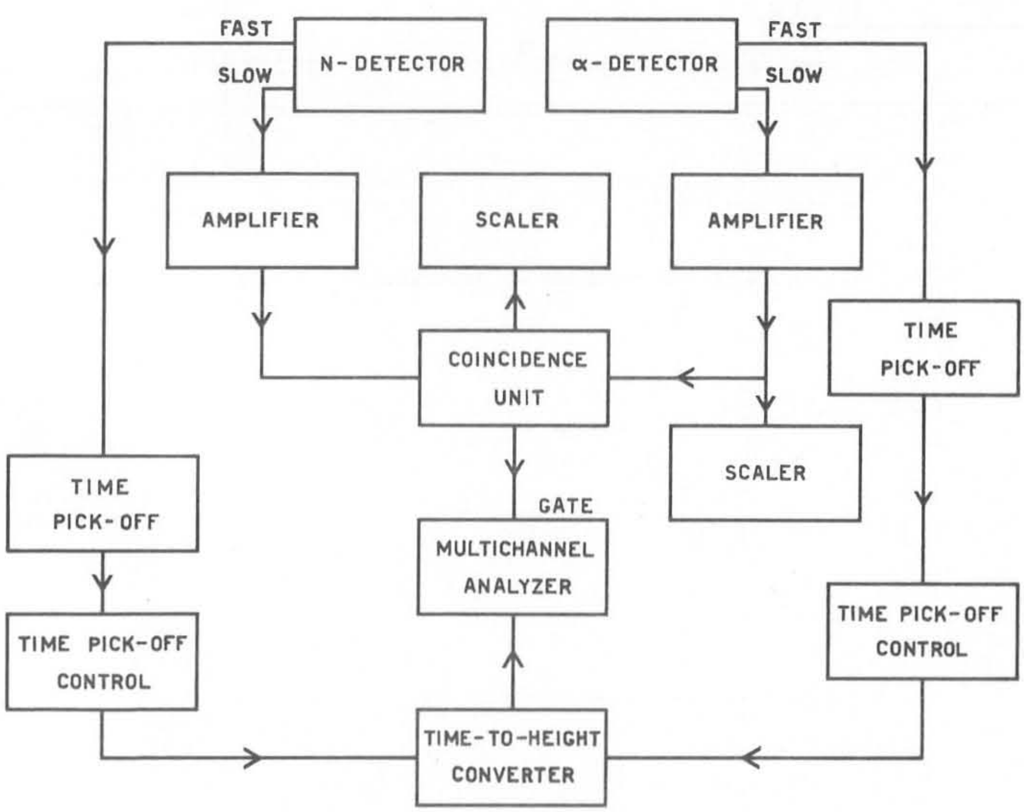

Fig. 11 - b) Block diagram of apparatus for the time-of-flight measuraments.

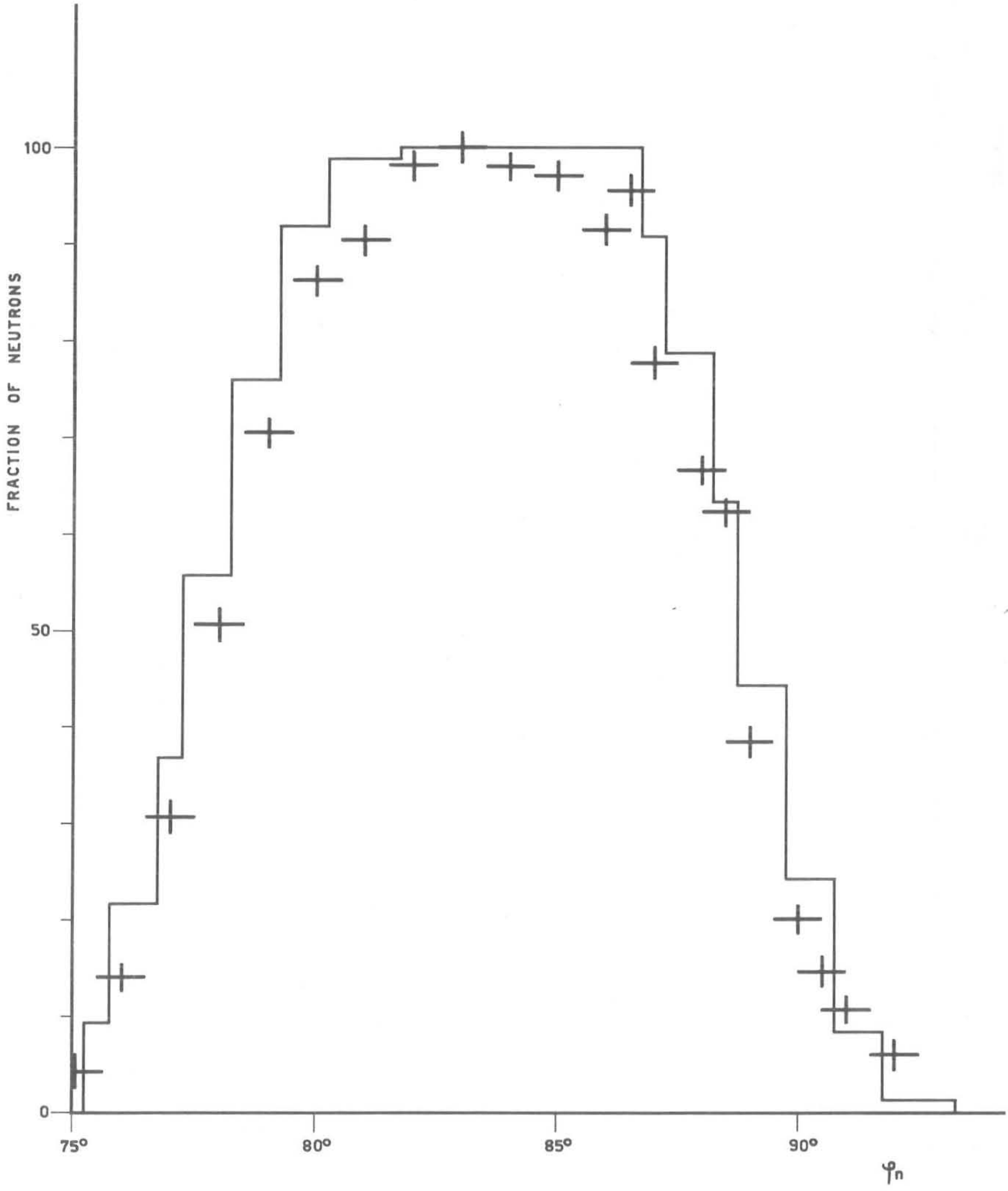

Fig. 12 - Comparison between the calculated shape of the correlated beam of neutrons and the measured one for $\Delta\varphi_\alpha = 5°30'$.

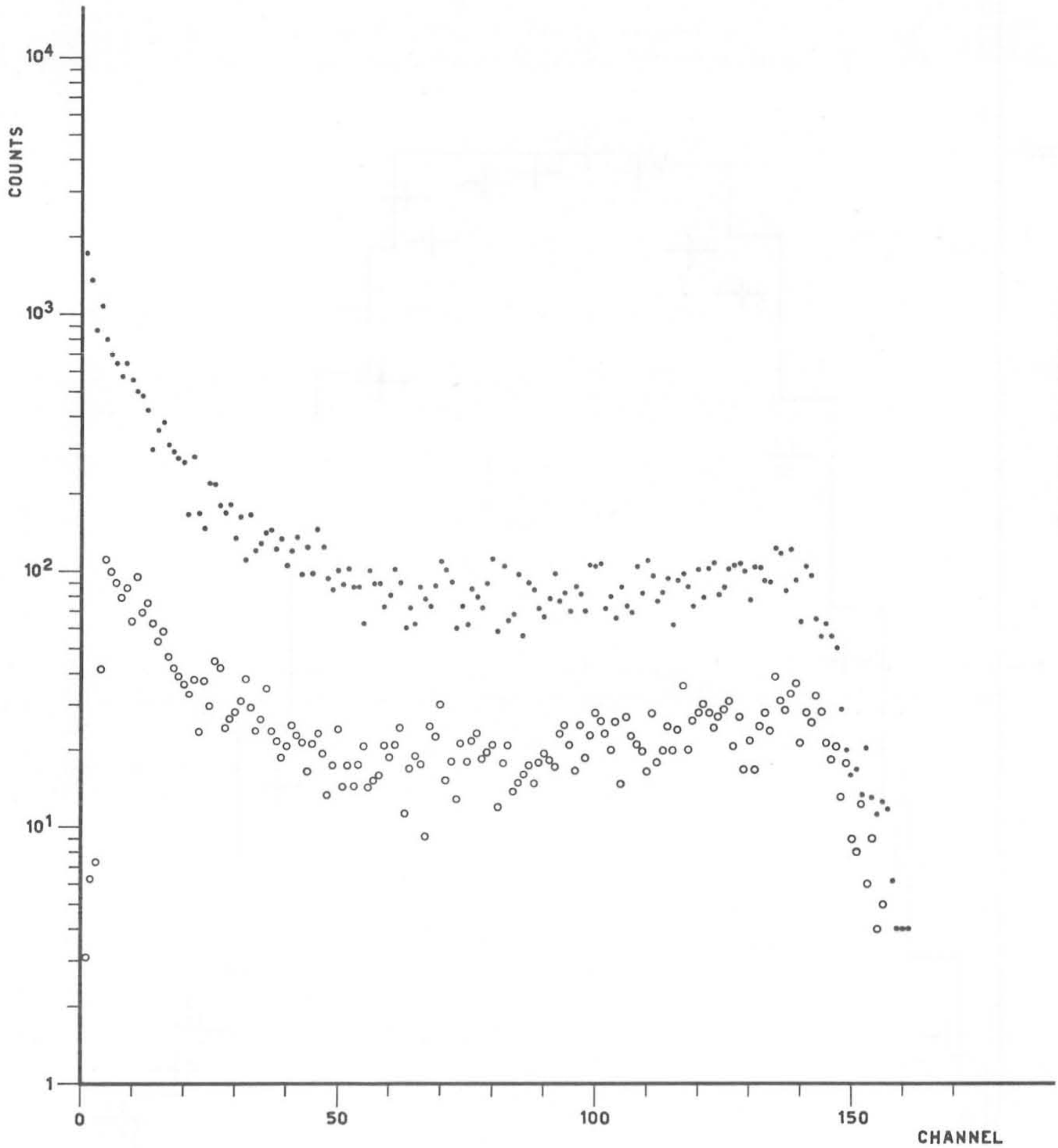

Fig. 13 - Spectra of neutrons (A: in coincidence, and B: not in coincidence) at 78° normalized to 10^7 α-particles.

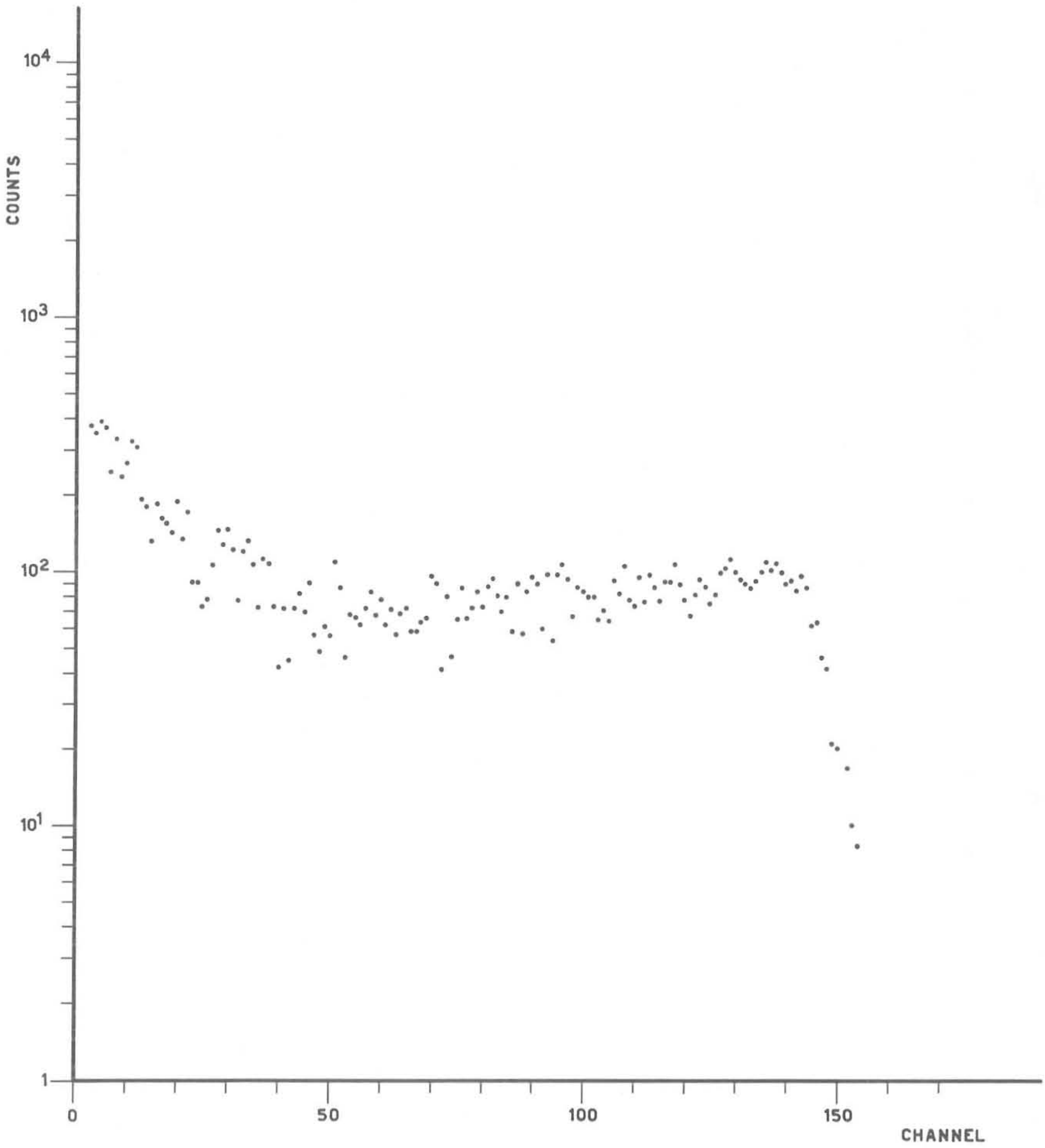

Fig. 14 a - Spectrum of neutrons detected with coincidence method at 84°, normalized to 10^7 α-particles.

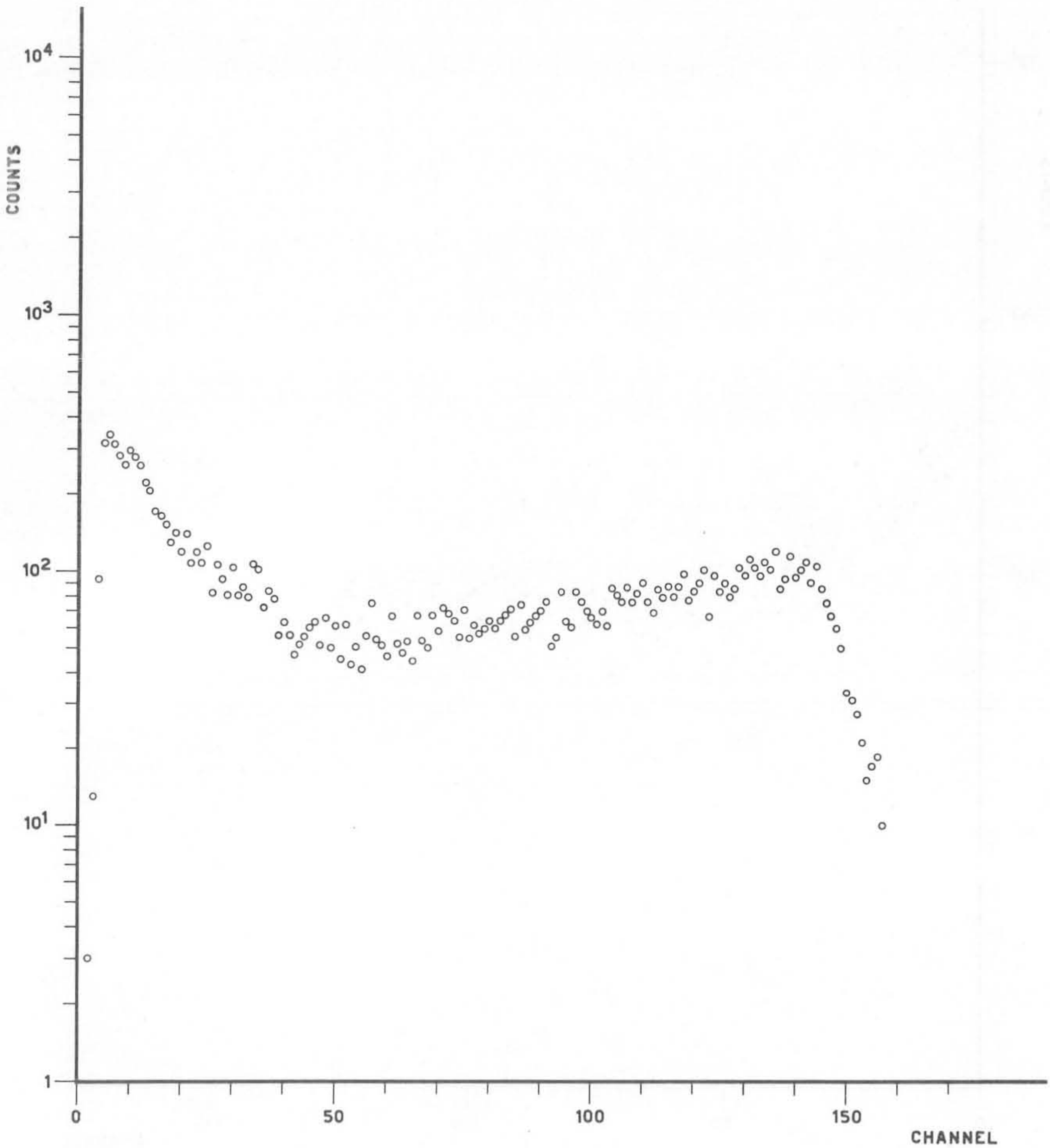

Fig. 14 b - Free spectrum at 84° normalized to 10^7 α-particles.

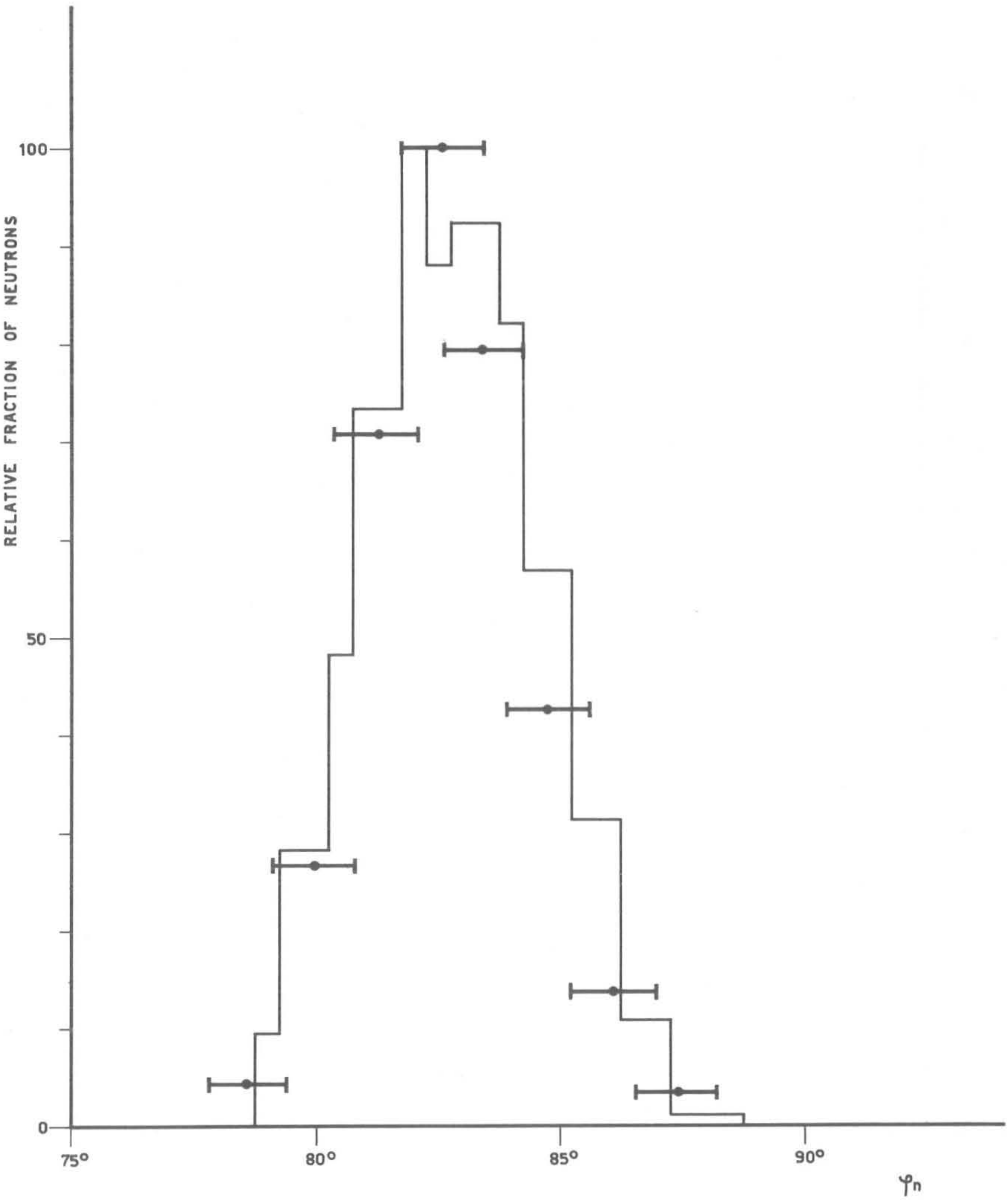

Fig. 15 - Comparison between the calculated and measured shapes of the beam. The histogram represents the calculated beam ($\Delta\varphi_\alpha$ = 1°45'). The points represent the measured beam ($\Delta\varphi_\alpha$ = 1°47').

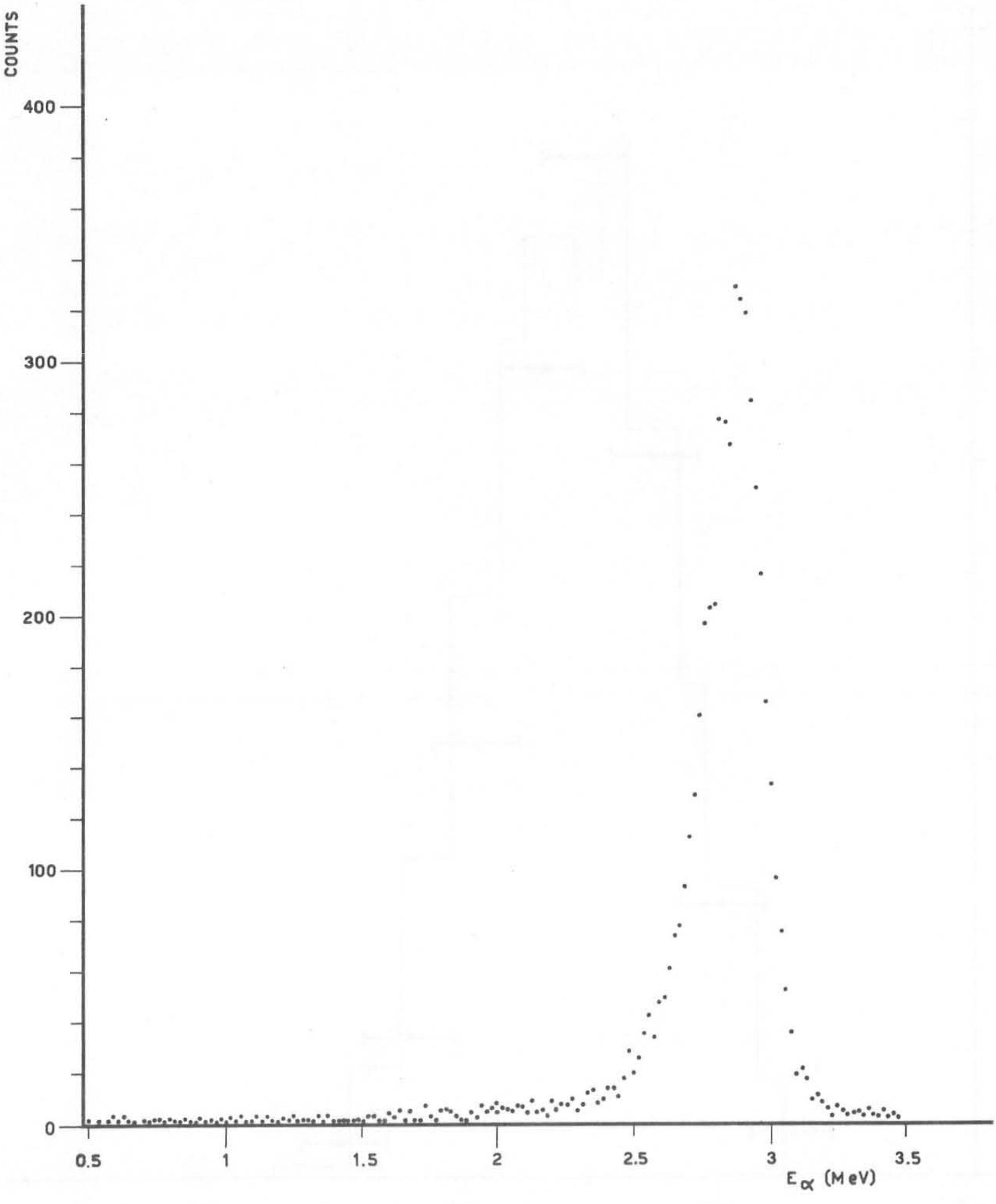

Fig. 16 - α-spectrum measured with a solid state detector. The energy of the incident deuterons is equal to 120 KeV.

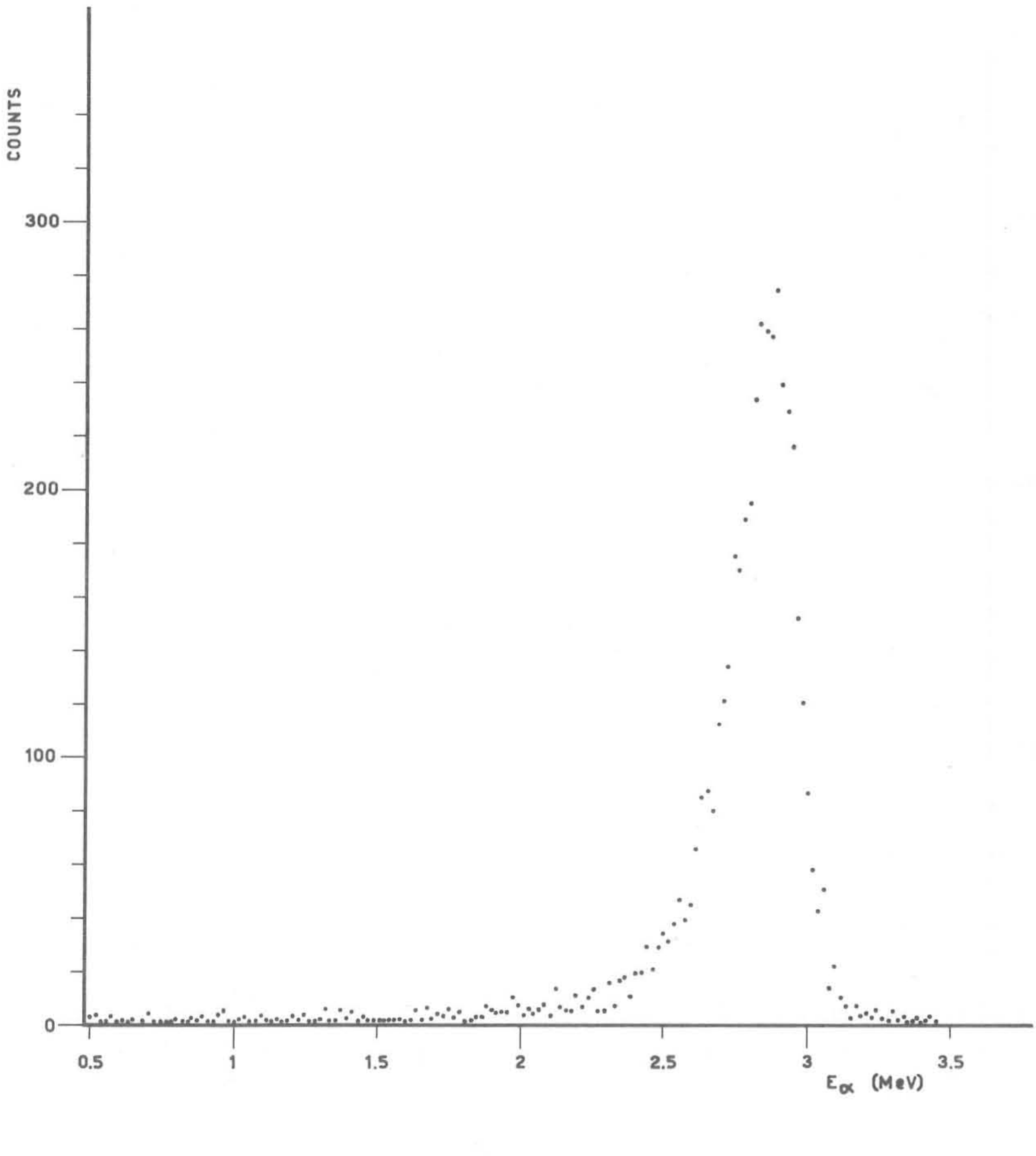

Fig. 17 - α-spectrum measured with a solid state detector. The energy of the incident deuterons is equal to 150 KeV.

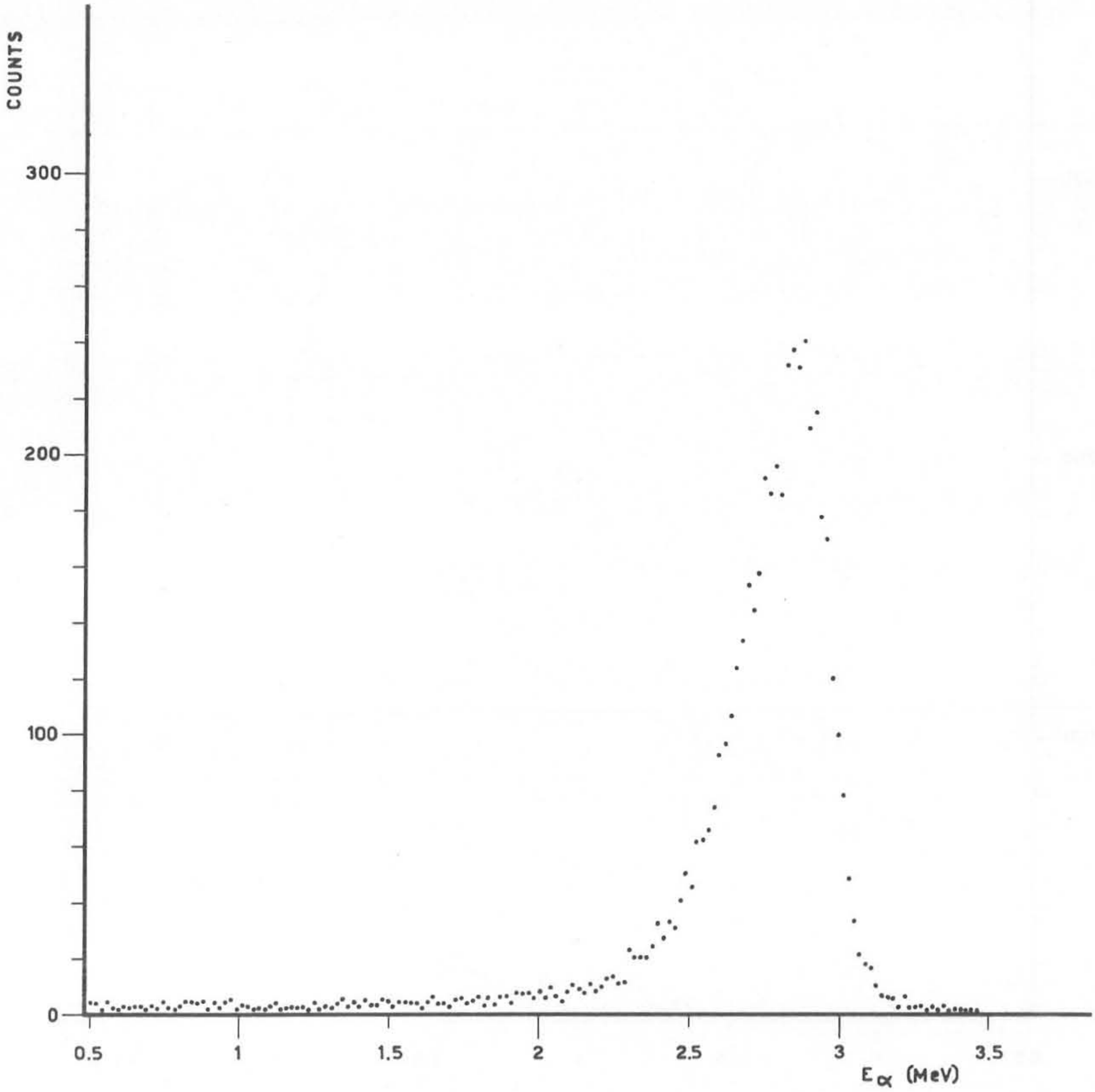

Fig. 18 - α-spectrum measured with a solid state detector. The energy of the incident deuterons is equal to 200 KeV.

A P P E N D I X

Listing of the computer programme in the case the α-particles are detected between 86°30' and 93°30'.

```
$IBFTC SARA
      DOUBLEPRECISION TRASM,ASSB,ARG1,ARG2
      DIMENSION ED(8),SIGMA(8),DEX1(8),DEX2(8),DEXM(8),DI(8),SIGMAD(8),
     1TRASM(8),SD(8),SDI(8),ASSB(8),PREC(8),PHI(8,100),TETAN(100),
     2TETANG(100),SUM(100)
      READ(5,999)(ED(I),I=1,8),(SIGMA(I),I=1,8),(DEX1(I),I=1,8),(DEX2(I)
     1,I=1,8)
999   FORMAT(8F6.3/8E10.3/8F6.3/8F6.3)
      RO1=382.
      RO2=4500.
      XN1=6.372E18
      XN2=4.900E18
      SPESSO=0.87E-04
      XNL=XN1/SPESSO
      ETA=XN1/XN2
      ROM=RO1+RO2
      DE=0.025
      WRITE(6,998)
998   FORMAT(1X,6HED MEV,3X,16HDEXM(MEV/MG/CM2),3X,6HDI(CM),3X,13HSD(BAR
     1N X CM),3X,5HTRASM,8X,12HASSORBIMENTO)
      DO 1 I=1,8
      DEXM(I)=(48.*DEX2(I)/(48.+3.*ETA)+3.*ETA*DEX1(I)/(48.+3.*ETA))
      DI(I)=(DE/DEXM(I))/ROM
      SD(I)=0.
      SDI(I)=0.
      DO 2 K=1,I
      SD(I)=SD(I)+SIGMA(K)*DI(K)
2     SDI(I)=SDI(I)+DI(K)
      ARG1=-XNL*SD(I)
      TRASM(I)=DEXP(ARG1)
      ARG2=-XNL*SIGMA(I)*DI(I)
      ASSB(I)=1.00-DEXP(ARG2)
1     WRITE(6,997) ED(I),DEXM(I),DI(I),SD(I),TRASM(I),ASSB(I)
997   FORMAT(1X,F6.3,3X,F6.3,9X,F8.5,1X,E10.3,6X,D11.4,3X,D11.4)
      ED(1)=0.200
      PERC(1)=(1.DO-TRASM(1))/(1.00-TRASM(8))
      WRITE(6,996)
996   FORMAT(1X,6HED MEV,3X22HCONTRIBUTO PERCENTUALE)
      WRITE(6,995) ED(1),PERC(1)
995   FORMAT(1X,F6.3,3X,E10.3)
      DO 3 I=2,8
      PERC(I)=(TRASM(I-1)*ASSB(I))/(1.00-TRASM(8))
3     WRITE(6,995) ED(I),PERC(I)
      DO 4 I=1,8
      WRITE(6,994) ED(I)
```

```
994   FORMAT(1X,21HENERGIA DEUTONI(MEV)=,F6.3//1X,15HANGOLO N(GRADI),3X,
     114HENERGIA N(MEV),3X,17HENERGIA ALFA(MEV),3X,18HANGOLO ALFA(GRADI)
     2,3X,19HENERGIA USCITA ALFA,3X,10HTEMPOV(NS),3X,3HPHI)
      TETAN(1)=69.*0.01745
      SALTO=.01745/2.
      AMD=2.014740
      AMN=1.008986
      AMA=4.003873
      Q=17.585832
      DO 4 K=1,100
      TETAN(K+1)=TETAN(K)+SALTO
      A=(SQRT(AMD*AMN*ED(I)*COS(TETAN(K)))/(AMN+AMA)
      B=(AMA*Q+ED(I)*(AMA-AMD))/(AMN+AMA)
      EN=(SQRT((A**2)+B)+A)**2
      EALFA=ED(I)+Q-EN
      DEXAT=-4.565*((ALOG(EALFA)+5.)/(EALFA))*1.E+01
      DEXATI=-7.450*((ALOG(EALFA)+2.151)/(EALFA))*1.E02
      DEXMI=(48.*DEXATI/(48.+3.*ETA)+3.*ETA*DEXAT/(48.+3.*ETA))
      DEALFA=DEXMI*SDI(I)
      REALFA=ELFA+DEALFA
      TEMPOV=(SQRT(AMA/(2.*REALFA*1.6)))*128.8
      TETAA=ARCOS(SQRT((AMD*ED(I))/(AMA*EALFA))-COS(TETAN(K))*SQRT((AMN*E
     1EN)/(AMA*EALFA)))
      TETANG(K)=TETAN(K)/0.01745
      TETAAG=TETAA/0.01745
      IF(TETAAG.LT.86.5) GO TO 5
      IF(TETAAG.GT.93.5) GO TO 5
      PHI(I,K)=PERC(I)
      WRITE(6,993)TETANG(K),EN,EALFA,TETAAG,REALFA,TEMPOV,PHI(I,K)
993   FORMAT(1X,F6.1,12X,F7.3,10X,F7.3,13X,F6.1,15X,F7.3,15X,F7.2,6X,
     1E10.3)
      GO TO 4
5     PHI(I,K)=0
4     CONTINUE
      WRITE(6,992)
992   FORMAT(1X,15HANGOLO N(GRADI),3X,24HFUNZIONE FASCIO NEUTRONI)
      DO 6 K=1,100
      SUM(K)=0.
      DO 7 I=1,8
7     SUM(K)=SUM(K)+PHI(I,K)
6     WRITE(6,991) TETANG(K),SUM(K)
991   FORMAT(1X,F6.1,12X,E10.3)
      END
```

R E F E R E N C E S

(1) E.M. Gunnersen and G. James, Nuclear Instruments and Methods 8 (1960) 173.

(2) W. Whaling, in Handbuch der Physik, Vol. 34, Ed. by S. Flügge; Springer-Verlog, Berlin (1958, p. 193.

(3) T.R. Fewell, Nuclear Instrument and Methods 61 (1968) 61.

(4) J.E. Bralley, J.R. and J.L. Fowler, in Fast Neutron Physics, Part.I, Ed. by J.B. Marion and J.L. Fowler; Interscience, London, (1960) p. 91.